Two-Photon Absorption Properties of Iron(II) and Ruthenium(II) Trischelate Complexes of 2,2′:4,4″:4′,4‴-Quaterpyridinium Ligands

Benjamin J. Coe,*,† Marek Samoc,*,‡ Anna Samoc,‡ Lingyun Zhu,§ Yuanping Yi,§ and Zhigang Shuai*,§

School of Chemistry, University of Manchester, Oxford Road, Manchester M13 9PL, UK, Laser Physics Centre, Research School of Physical Sciences and Engineering, Australian National University, Canberra ACT 0200, Australia, and Key Laboratory of Organic Solids, Institute of Chemistry, Chinese Academy of Sciences, Beijing 100080, China

Received: August 29, 2006; In Final Form: November 1, 2006

A series of Ru^{II} or Fe^{II} trischelate complex salts containing *N*-methyl/aryl-2,2′:4,4″:4′,4‴-quaterpyridinium ligands that has previously been subjected to quadratic nonlinear optical studies (Coe, B. J. et al. *J. Am. Chem. Soc.* **2005**, *127*, 13399) has now been investigated for two-photon absorbing behavior. Z-scan measurements using a 750 nm laser afford reasonably large two-photon absorption (2PA) cross-sections σ_2 of ca. 62−180 GM for the Ru^{II} complexes, but only very weak 2PA is observed for the Fe^{II} compounds. The excited-state and 2PA properties of the representative chromophore $[Ru^{II}(Me_2Qpy^{2+})_3]^{8+}$ (Me_2Qpy^{2+} = *N*″,*N*‴-dimethyl-2,2′:4,4″:4′,4‴-quaterpyridinium) have also been investigated by using semiempirical intermediate neglect of differential overlap/multireference-determinant single and double configuration interaction computations with the optimized geometry obtained via density functional theory. The calculated σ_2 value of ca. 624 GM at 1.70 eV for this metal-to-ligand charge-transfer chromophore is about 10 times larger than that obtained from the Z-scan studies.

Introduction

Organic nonlinear optical (NLO) materials have been extensively investigated over recent years, largely because of their promise in a wide range of interesting technological applications.[1] Quadratic (second-order) NLO effects are suited to various opto-electronic applications, while cubic (third-order) phenomena are relevant to all-optical data processing and applications in nanophotonics and biophotonics. A broad range of chromophores has been found to display large molecular NLO responses, represented by first and second hyperpolarizabilities (β and γ), from which derive quadratic and cubic effects, respectively. Beyond purely organic NLO compounds, transition metal complexes are particularly interesting because of their structural diversity and multifunctional nature.[2] The promise of metal complexes in this field is exemplified by recent demonstrations of the reversible switching of both quadratic and cubic NLO responses via metal-based redox processes.[3]

Molecules with large two-photon absorption (2PA) cross-sections σ_2 are of major interest for a wide range of potential applications, including optical power limiting, two-photon upconversion lasing, and photodynamic cancer therapy.[4] The quantity σ_2 is related to the imaginary part of the cubic NLO response γ. It is established that large σ_2 values require extended conjugated π-systems and recent studies have featured a number of branched structures, including octupolar chromophores.[5] Only very few 2PA studies have involved octupolar metal complexes,[3i,6] but Liu et al. have recently used INDO/SOS calculations to predict extremely large σ_2 values for octupolar Cu^{I} and Zn^{II} 2,2′-bipyridyl (bpy) complexes with tetrahedral or octahedral geometries.[7] One of the reasons for the relative scarcity of reports of σ_2 measurements on octupolar metal complexes is that they are often not fluorescent and thus cannot be studied by the convenient technique of two-photon induced fluorescence. We have previously reported studies on the quadratic NLO properties of Ru^{II} trisbpy derivatives,[8] and describe here the results of 2PA measurements and computational studies on these complex species.

Experimental Section

Materials. The complex salts **1**−**7** were prepared as described previously,[8] and the complex salt $[Ru^{II}(Qpy)_3](PF_6)_2$ (**8**, Qpy = 2,2′:4,4″:4′,4‴-quaterpyridyl) was synthesized according to a published procedure.[9]

Z-Scan Measurements. All compounds were investigated as DMF solutions placed in 1 mm path length glass cells. The measurements were carried out at 750 nm (1.652 eV). This wavelength was chosen in such a way as to provide the optimum possible enhancement of the NLO properties of the compounds while avoiding excessive one-photon absorption. The laser system used for the measurements used a Clark-MXR regenerative amplifier operating at 250 Hz and generating ca. 700 μJ pulses at 775 nm, which were used to pump a Light Conversion TOPAS travelling wave optical parametric amplifier. The wavelength for the present measurements was obtained by doubling the OPA signal.

A standard Z-scan measurement system was used with the beam from the OPA being first attenuated and spatially filtered

* Corresponding authors. (B.J.C.) E-mail: b.coe@manchester.ac.uk. Tel: +44 161 275 4601. Fax: +44 161 275 4598. (M.S.) E-mail: marek.samoc@anu.edu.au. Tel: +02 6125 4611. Fax: +02 6125 0029. (Z.S.) E-mail: zgshuai@iccas.ac.cn. Tel: +86 10 62521934. Fax: +86 10 62525573.

† University of Manchester.

‡ Australian National University.

§ Chinese Academy of Sciences.

10.1021/jp0656072 CCC: $37.00
Published on Web 12/29/2006

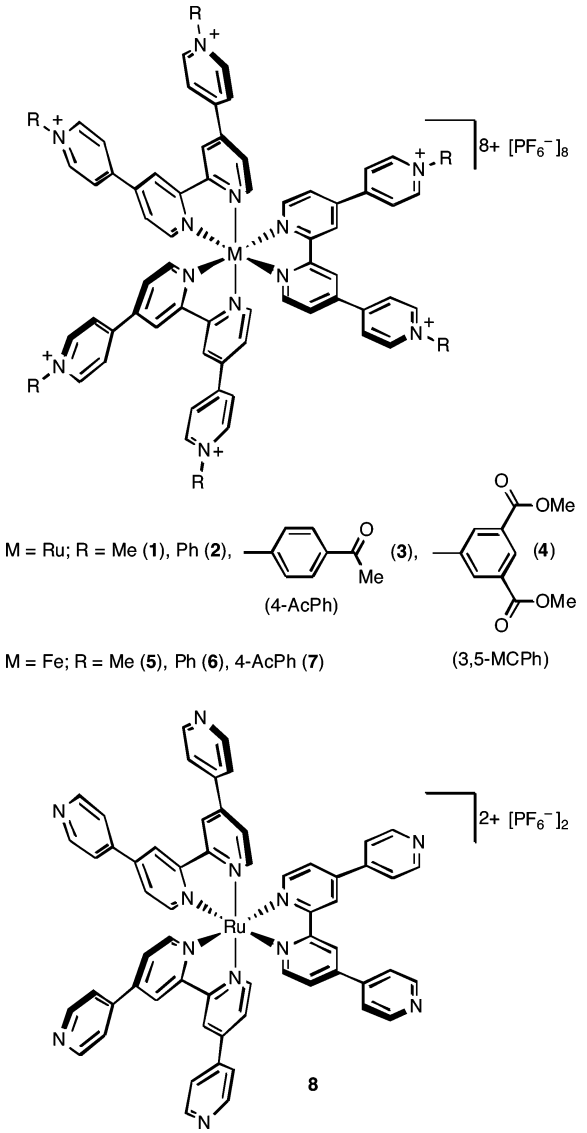

Figure 1. Chemical structures of the complex salts investigated.[8,9]

TABLE 1: Nonlinear Optical Parameters at 750 nm

salt	γ_{real} (10^{-36} esu)	γ_{imag} (10^{-36} esu)	σ_2 (GM)[a]
1	-4300 ± 600	220 ± 30	62 ± 8
5	-7400 ± 800	48 ± 15	13 ± 4
2	-5800 ± 1500	420 ± 100	120 ± 25
6	-6400 ± 1500	13 ± 6	3.6 ± 2
3	-6700 ± 2000	660 ± 150	180 ± 30
7	-6600 ± 2000	21 ± 10	5.8 ± 3
4	-5600 ± 1500	330 ± 80	92 ± 20
8	-380 ± 150	18 ± 10	5.0 ± 3

[a] 1 GM = 10^{-50} cm^4 s.

by a pair of apertures and then focused with a lens to form a $w_0 = 60$ μm spot at the focal plane (i.e., $z = 0$). The cell was mounted on a travelling stage that was moved from $z = -47.5$ to $z = 47.5$ mm. The beam transmitted through the sample was probed with a beam splitter to provide an "open aperture" signal and with an iris aperture in the far field to provide the "closed aperture" signal simultaneously. The Z-scans were analyzed using home-written software implementing the calculations of Z-scans as presented by Sheik-Bahae et al.[10]

By comparing the shapes of computed curves with the experimental ones, we obtained the values of the nonlinear phase

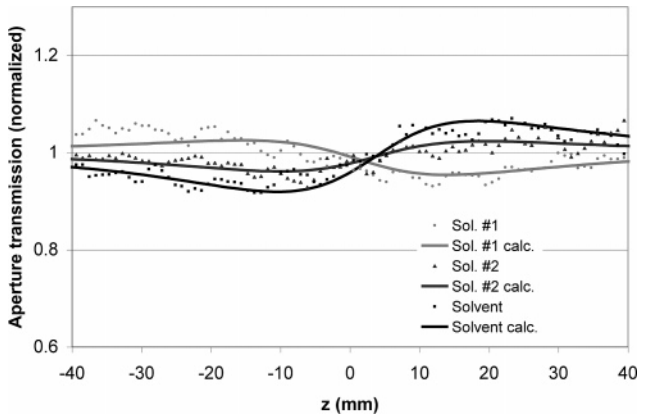

Figure 2. Examples of closed-aperture Z-scans for compound **1** in DMF. Sol. #1 = 3.13%, Sol. #2 = 1.50%. Beam parameters: $w_0 = 65$ μm.

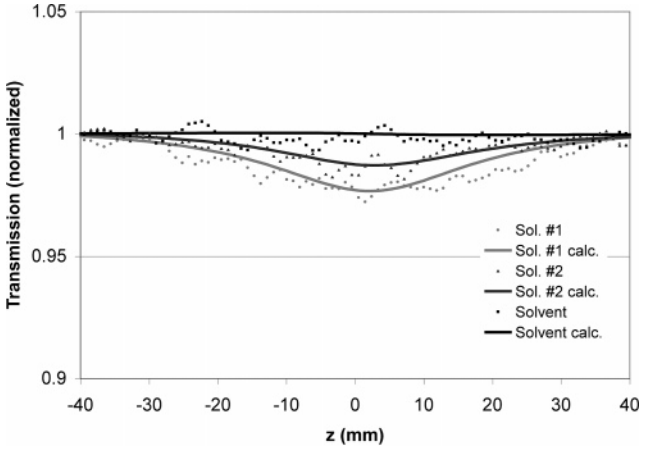

Figure 3. Examples of open-aperture Z-scans for compound **1** in DMF. Sol. #1 = 3.13%, Sol. #2 = 1.50%. Beam parameters: $w_0 = 65$ μm.

shift $\Delta\Phi_0$ [= Re($\Delta\hat{\Phi}_0$)] and the T factor defined here according to the equation

$$T = 4\pi \frac{\mathrm{Im}(\Delta\hat{\Phi}_0)}{\mathrm{Re}(\Delta\hat{\Phi}_0)} \quad (1)$$

where $\Delta\hat{\Phi}_0$ stands for the complex phase shift. All measurements were performed in the range of intensities at which the phase shifts were below ca. 1 rd. The Z-scans were measured for three concentrations of each compound in DMF (the highest concentration being typically about 4 wt %) as well as for the solvent itself, and the NLO properties of the solute were determined assuming linear dependences of the phase shift on concentration. The data were calibrated against the nonlinearity of fused silica that was taken to be $n_2 = 3 \times 10^{-6}$ cm^2 W^{-1}.

Computational Methodology. As described previously,[8] the geometry of the representative complex cation in salt **1** was optimized at the B3P86/LanL2DZ level, restricted to D_3 symmetry, implemented in the Gaussian 03 program.[11] The standard orientation of the molecule places the z-axis aligned to the C_3 axis and the y-axis aligned to one of the C_2 axes.

The semiempirical intermediate neglect of differential overlap (INDO)[12] Hamiltonian with Mataga−Nishimoto (MN)[13] potential was used to investigate the excited-state properties as well as the 2PA coefficients. On the basis of the ZINDO parameters, we have implemented a multireference-determinant single and double configuration interaction technique (MRD−CI)[14] scheme.

The CI active space in our MRD−CI calculation consists of 11 HOMOs and 11 LUMOs and 5 references, amounting to a total of about 130 000 configurations. A Davidson diagonalization algorithm is followed to obtain a few hundred lowest-lying excited states. We note that in the standard ZINDO calculations, only 2 occupied and 2 unoccupied MOs have been considered in such calculations for the 2PA properties and only 200 configurations are included in the CI calculations, meaning that many important molecular orbitals as well as configuration contributions have been ignored.[15] Previously an extended version of the ZINDO program has been successfully applied to calculate the NLO properties and multiphoton absorptions, which allowed up to 6000 configurations or 6 occupied−6 unoccupied active MO space.[16]

To calculate the 2PA cross-sections, we have used the tensor approach including the 130 lowest lying excited singlet states in the perturbative description. The 2PA cross-section, $\sigma_2(\omega)$, can be expressed according to the relationship[17]

$$\sigma_2(\omega) = \frac{4\pi^3(\hbar\omega)^2L^4}{n^2c^2\hbar}\sum_f |S^{ij}_{g\to f}|^2 \cdot \left\{\frac{\Gamma}{(E_{gf}-2\hbar\omega)^2+\Gamma^2}\right\} \quad (2)$$

where c is the speed of light in a vacuum, L denotes a local-field correction (equal to 1 for vacuum), $\hbar\omega$ is the photon energy of the incident light (a degenerate 2PA process is assumed), and Γ is a Lorentzian broadening factor (set to 0.1 eV in the calculations). $S_{g\to f}$ corresponds to the two-photon transition amplitude from the ground state to a final three-photon state $|f\rangle$, with tensor ij component defined as

$$S^{ij}_{g\to f} = \sum P_{ij}\sum_m \frac{< g|\mu_i|m > < m|\mu_j|f >}{(E_{gm}-\hbar\omega - i\Gamma)} \quad (3)$$

where E_{gm} corresponds to the excitation energy from the ground state $|g\rangle$ to excited state $|m\rangle$, μ_i is the component of the electric dipole operator along the molecular axis i and P_{ij} denotes a complete permutation of the indices i and j. For linearly polarized light, the average 2PA cross-section can be written as[18]

$$\sigma_2(\omega) = \frac{4\pi^3(\hbar\omega)^2L^4}{n^2c^2\hbar(15)}\sum_f |\sum_{ij} S^{ii}_{g\to f}(S^{jj}_{g\to f}{}^*) + 2\sum_{ij} S^{ij}_{g\to f}S^{ij}_{g\to f}{}^*| \cdot \left\{\frac{\Gamma}{(E_{gf}-2\hbar\omega)^2+\Gamma^2}\right\} \quad (4)$$

Results and Discussion

Experimental Studies. The real and imaginary parts of γ obtained for all of the compounds studied (structures shown in Figure 1) are listed in Table 1. Figure 2 shows examples of closed aperture Z-scans (for compound **1**) and Figure 3 shows examples of open aperture scans. Strong negative refractive nonlinearities (γ_{real}) of all compounds are likely to be related to the presence of absorption: one-photon absorption in the case of the Fe^{II} complexes in **5**−**7** and 2PA in the case of the Ru^{II} complexes in **1**−**4** and **8**. Within the experimental error, there is only a very weak signature of any 2PA for the Fe^{II} compounds, whereas all of the Ru^{II} compounds are relatively efficient two-photon absorbers.

The data in Table 1 reveal a 2-fold increase in σ_2 for the ruthenium complexes on moving from **1** to **2**, most likely attributable to extension of the size of the conjugated system. The addition of substituents on the terminal phenyl rings further modifies the value of σ_2. However, from comparison of the results for **3** and **4**, it is not clear if the observed variations in σ_2 for **1**−**4** are due to changes in the conjugation or changes in the multipolar character of the complexes. The comparison between **1**−**4** and **8** accentuates the role of the multipolar charge distribution in the complex in attaining strong cubic NLO behavior, because all of the pyridinium compounds show 2PA that is at least an order of magnitude stronger than that in the unquaternised complex in **8**. In contrast, no significant 2PA is detected for the iron complexes in **5**, **6**, and **7** and no trend in cubic optical nonlinearity is evident for these three compounds. The refractive component of the cubic optical nonlinearity of **5, 6**, and **7** is the same for the three complexes within the experimental error. The much weaker 2PA behavior of the iron complexes when compared with their ruthenium analogues may be attributable at least in part to the higher polarizability of the latter due to the greater radial extension of the 4d as opposed to 3d orbitals.

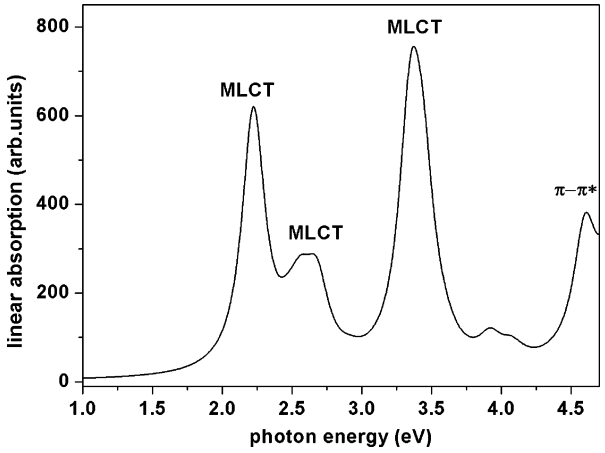

Figure 4. The INDO/MRD−CI calculated linear absorption spectrum of the complex cation in salt **1**.

TABLE 2: INDO/MRD−CI Calculated Excitation Energies, Transition Dipole Moments, Dipole Moment Changes, and the Most Significant CI Contributions to the Excited States for the Complex in 1

E_{max}(eV) theo [exp][a]	excited state (energy, eV)	CI description (weights > 0.3), character	M_{ge} (D)	$\|\Delta\mu_{ge}\|$ (D)
2.21	S_1 (2.21)	$0.93\|H\to L\rangle$, MLCT	5.40	1.06
[2.55]	S_2 (2.22)	$0.93\|H-1\to L\rangle$, MLCT	5.23	1.42
2.57−2.66	S_6 (2.56)	$0.75\|H\to L+1\rangle + 0.47\|H-1\to L+2\rangle$	3.47	1.92
[3.15]		$-0.31\|H-2\to L+2\rangle$, MLCT		
	S_7 (2.67)	$0.93\|H\to L+2\rangle$, MLCT	3.07	8.04
	S_8 (2.69)	$0.95\|H-1\to L+1\rangle$, MLCT	2.75	8.78
3.38	S_{10} (3.34)	$0.85\|H\to L+5\rangle + 0.30\|H\to L+10\rangle$, MLCT	4.40	2.08
[3.83]	S_{11} (3.35)	$-0.83\|H-1\to L+5\rangle + 0.28\|H-2\to L+4\rangle$, MLCT	4.64	1.17
	S_{12} (3.37)	$0.89\|H-2\to L+3\rangle$, MLCT	2.90	7.96
	S_{13} (3.37)	$0.86\|H-2\to L+4\rangle$, MLCT	2.38	7.80
	S_{14} (3.44)	$0.72\|H\to L+4\rangle + 0.60\|H-1\to L+3\rangle$, MLCT	5.53	0.72
4.61	S_{28} (4.60)	$0.64\|H-4\to L\rangle + 0.55\|H-10\to L\rangle$, $\pi\to\pi^*$	3.64	0.62
[4.81]	S_{29} (4.60)	$-0.64\|H-3\to L\rangle - 0.55\|H-9\to L\rangle$, $\pi\to\pi^*$	3.63	0.14

[a] Experimental data for acetonitrile solutions at 295 K taken from ref 8.

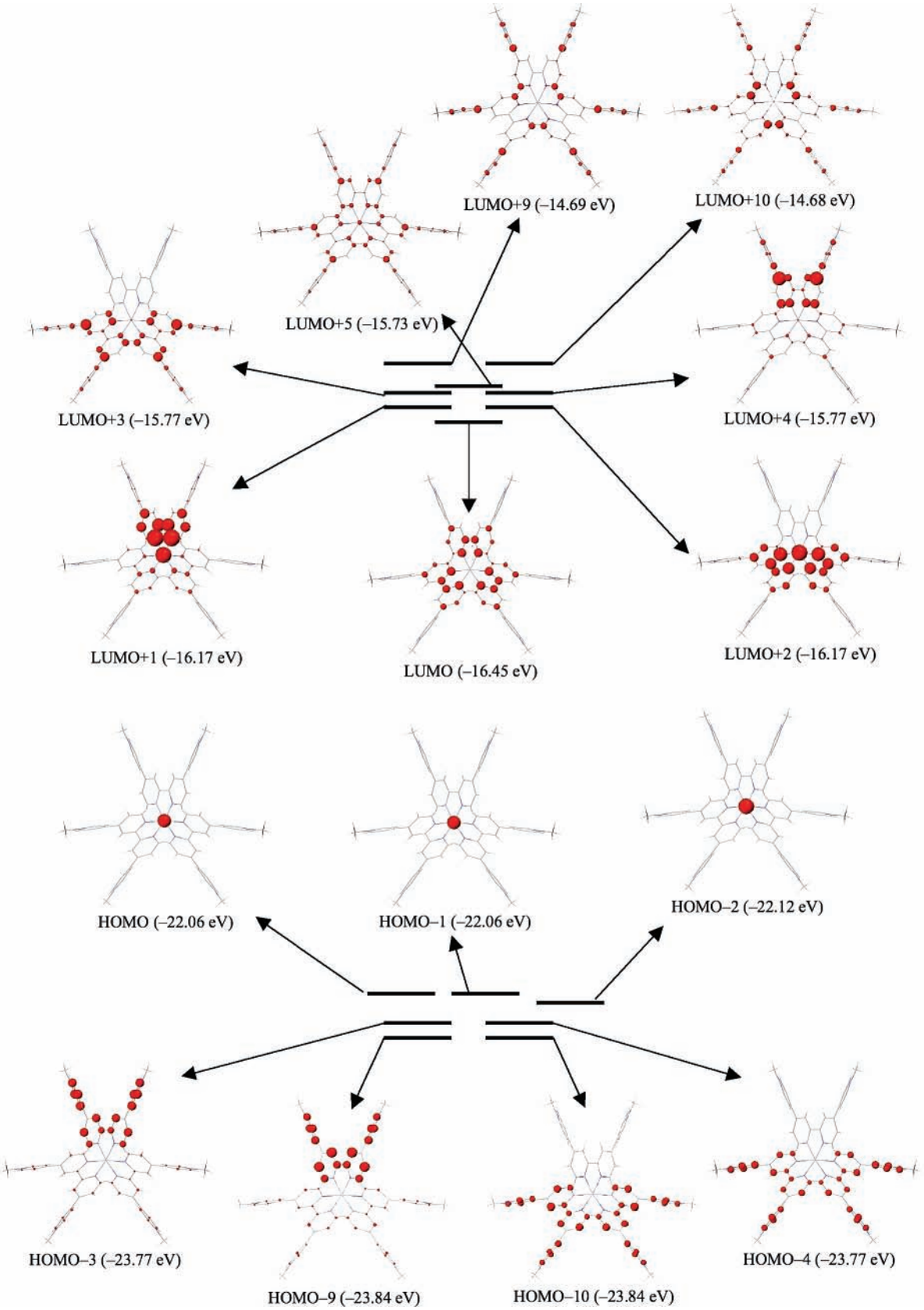

Figure 5. The electronic density distribution of the frontier molecular orbitals of the complex cation in salt **1**. For the sake of clarity, the electronic density is magnified by a relative ratio of 10, except for the HOMO, HOMO−1, and HOMO−2 orbitals.

Theoretical Studies: Linear Absorption. The INDO/MRD−CI calculated linear electronic absorption spectrum of the complex in salt **1** is shown in Figure 4 , and in Table 2 the excitation energies and transition dipoles and the most significant contributions to the CI description of the excited states are listed. The relevant orbitals are depicted in Figure 5. Unfortunately, at present we cannot generate meaningful theoretical results for complexes such as that in **5** because the INDO parametrization for iron is very poor. Test calculations on this chromophore have been carried out, but these could not reproduce the low-

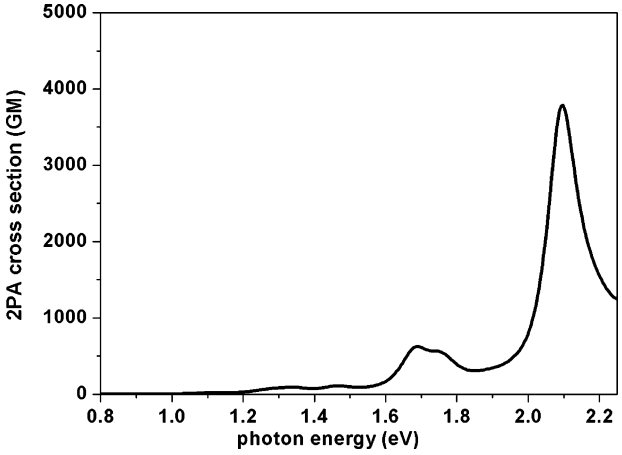

Figure 6. INDO/MRD−CI calculated 2PA spectrum of the complex cation in salt **1**.

lying excitation behavior. To use this approach to reliably calculate the linear absorption and 2PA properties of iron complexes, reparameterization will be necessary, which is a major undertaking and therefore outside the scope of our present studies.

The calculations on the complex in salt **1** indicate that four major peaks dominate the spectrum: (i) The first peak at 2.21 eV is associated with S_1 (2.21 eV) and S_2 (2.22 eV), two nearly degenerate excited states, which are dominated by excitations from the degenerate occupied HOMO and HOMO−1 to the unoccupied LUMO. The HOMO and HOMO−1 are mainly localized on the Ru^{II} center, while the LUMO is concentrated on the bipyridyl rings, indicating that this first peak has metal-to-ligand charge-transfer (MLCT) character. (ii) The second peak with a shoulder around 2.57−2.66 eV arises from the S_6, S_7, and S_8 excited states. These excitations are mainly from the degenerate HOMO and HOMO−1 to the degenerate LUMO+1 and LUMO+2, meaning that these three transitions also have MLCT character. (iii) The third peak at ca. 3.38 eV corresponds to the S_{10}, S_{11}, S_{12}, S_{13}, and S_{14} excited states, also possessing MLCT character. (iv) The fourth peak at ca. 4.61 eV involves the degenerate S_{28} and S_{29} excited states and has intraligand $\pi \rightarrow \pi^*$ character. The CI descriptions for both of these states are dominated by one-electron excitations to the LUMO from the degenerate pairs HOMO−3/HOMO−4 and HOMO−9/HOMO−10. HOMO−3, HOMO−4, HOMO−9 and HOMO−10 are distributed on the ligands with significant electron density on the pyridinium rings.

The experimentally measured absorptions for **1** in acetonitrile solution are found at 2.55, 3.15, 3.83, and 4.81 eV, with the two lowest energy bands assigned as having MLCT character.[8] There is hence a reasonable level of overall agreement between the measured and INDO/MRD−CI calculated data, with the main difference being that the calculated excitation energies are all substantially smaller than the experimental ones. This result may be because of solvent and vibronic coupling effects that are not considered in the present calculations. Interestingly, time-dependent density functional theory predicts energies of 2.78 and 3.26 eV for the MLCT transitions of the complex in salt **1**,[8] showing a closer agreement with the situation observed in acetonitrile solution when compared with the present INDO/MRD−CI calculations.

Theoretical Studies: Two-Photon Absorption. The INDO/MRD−CI calculated 2PA spectrum of the complex cation in salt **1** is shown in Figure 6. This spectrum is dominated by two absorption peaks, a low-energy peak at ca. 1.70 eV and a high-energy one at ca. 2.10 eV. The energy of the latter is close to the one-photon energy of the first linear absorption peak (2.21 eV); this band overlaps with the linear absorption and therefore is not useful for practical applications. Hence, we will only discuss 2PA in the spectral region below linear absorption, i.e., the low-energy peak at ca. 1.70 eV, which is associated with five close-lying excited states, S_{10}, S_{11}, S_{12}, S_{13}, and S_{14}, located at ca. 3.4 eV. The electronic transitions for these five excited states are of MLCT character with no $\pi \rightarrow \pi^*$ intraligand charge-transfer (ILCT) contributions due to the presence of the electron-accepting pyridinium substituents. The calculated σ_2 value at 1.70 eV is ca. 624 GM, and is about 10 times larger than that obtained from Z-scan studies (see above) at 1.652 eV, but still relatively small when compared with those of previously investigated 2PA chromophores containing large π-electronic systems.[6b,c,19] For the sake of comparison, we also have computed σ_2 from the SOS expression,[20] which amounts to ca. 640 GM at a photon energy of 1.70 eV. Therefore, the two theoretical approaches give very similar results.

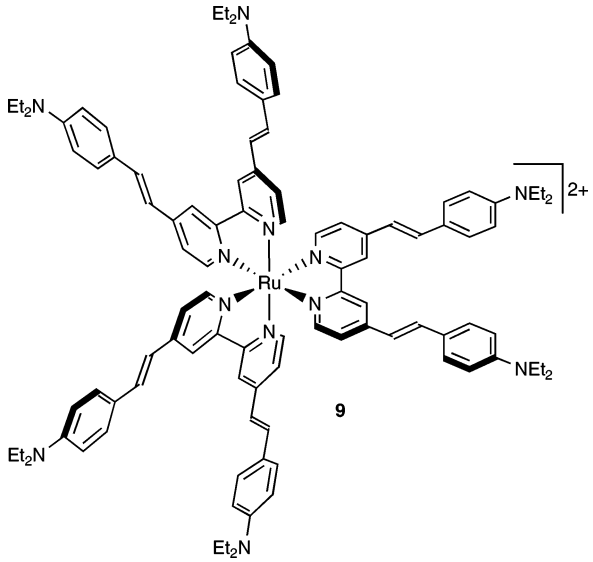

Figure 7. Chemical structure of a complex chromophore investigated by other workers.[21]

It is worth considering the reasons why the octupolar complex cation in salt **1** has only a relatively small σ_2 value despite its polyaromatic nature. Because this chromophore has no inversion symmetry, there is no parity restriction for either one- or two-photon absorption so the one-photon excited states may become two-photon active. The detuning energy, $E_{ge} - \hbar\omega$ of ca. 1.7 eV is quite large, and the transition dipole moments M_{ge} from the ground state to these five excited states are relatively small (i.e., 4.40 D for $S_0 \rightarrow S_{10}$, 4.64 D for $S_0 \rightarrow S_{11}$, 2.90 D for $S_0 \rightarrow S_{12}$, 2.38 for $S_0 \rightarrow S_{13}$, and 5.53 D for $S_0 \rightarrow S_{14}$ (Table 2)). In contrast, similar calculations predict that the related complex chromophore **9** (Figure 7), which has been studied for its quadratic NLO properties by Le Bozec and co-workers,[21] should possess a much larger σ_2 value of ca. 20 000 GM. The electronic absorption spectrum of this and related complexes are dominated by intense ILCT transitions that arise from the presence of peripheral electron-donating substituents. Hence, it is apparent that such species display much greater promise for potential 2PA applications than related MLCT-based chromophores.

The difference between the magnitudes of the computed σ_2 values and that obtained from Z-scan measurements on salt **1** (Table 1) may originate from several factors. As discussed previously,[22] calculated σ_2 values may be substantially overestimated if Franck−Condon factors of the vibrational transitions

and the related broadening of the absorption profiles are not properly accounted for. In addition, 2PA measurements performed at only a single wavelength do not provide certainty that the maximum value of σ_2 in a given 2PA band has been reached. Nevertheless, the present experimental and computational data provide information that should be helpful in the future design of metal complexes displaying enhanced nonlinear absorption properties.

Conclusions

Z-scan measurements using a 750 nm laser show that Ru^{II} trischelate complexes of *N*-methyl/aryl-2,2′:4,4″:4′,4‴-quaterpyridinium ligands show moderate 2PA cross-sections σ_2 of ca. 62−180 GM. In contrast, analogous Fe^{II} compounds display only very weak 2PA behavior. Semiempirical INDO/MRD−CI computations on the representative *N*-methylated chromophore in salt **1** shed light on the excited-state and 2PA properties, affording a predicted σ_2 value of ca. 624 GM at 1.70 eV that is about 10 times larger than that measured. The relatively inefficient 2PA behavior of the Ru^{II} complexes (when considering their polyaromatic nature) can be attributed at least in part to the modest intensities of their visible MLCT transitions, and related chromophores in which the one-photon absorption spectra are dominated by more strongly allowed ILCT excitations are predicted to possess much larger σ_2 values.

Acknowledgment. We thank the EPSRC for support (Grant GR/M93864) and also the Australian Research Council (Grant DP0556942). The work in Beijing is supported by NSFC (Grant No. 20420150034, 20433070, 10425420) and the numerical calculations were carried out in the supercomputer center of the Chinese Academy of Sciences.

References and Notes

(1) (a) *Nonlinear Optical Properties of Organic Molecules and Crystals*; Chemla, D. S., Zyss, J., Eds.; Academic Press: Orlando, FL, 1987; Vols. 1 and 2. (b) Zyss, J. *Molecular Nonlinear Optics: Materials, Physics and Devices*; Academic Press: Boston, MA, 1994. (c) Bosshard, Ch., Sutter, K., Prêtre, Ph., Hulliger, J., Flörsheimer, M., Kaatz, P., Günter, P.; *Organic Nonlinear Optical Materials* (*Advances in Nonlinear Optics*); Gordon & Breach: Amsterdam, The Netherlands, 1995; Vol. 1. (d) *Nonlinear Optics of Organic Molecules and Polymers*; Nalwa, H. S., Miyata, S., Eds.; CRC Press: Boca Raton, FL, 1997. (e) Marder, S. R. *Chem. Commun.* **2006**, 131. (f) *Nonlinear Optical Properties of Matter: From Molecules to Condensed Phases*; Papadopoulos, M. G.; Leszczynski, J.; Sadlej, A. J., Eds.; Springer: Dordrecht, The Netherlands, 2006.

(2) (a) Kanis, D. R.; Ratner, M. A.; Marks, T. J. *Chem. Rev.* **1994**, *94*, 195. (b) Long, N. J. *Angew. Chem., Int. Ed. Engl.* **1995**, *34*, 21. (c) Whittall, I. R.; McDonagh, A. M.; Humphrey, M. G.; Samoc, M. *Adv. Organomet. Chem.* **1998**, *42*, 291. (d) Whittall, I. R.; McDonagh, A. M.; Humphrey, M. G.; Samoc, M. *Adv. Organomet. Chem.* **1998**, *43*, 349. (e) Heck, J.; Dabek, S.; Meyer-Friedrichsen, T.; Wong, H. *Coord. Chem. Rev.* **1999**, *190*−*192*, 1217. (f) Gray, G. M.; Lawson, C. M. In *Optoelectronic Properties of Inorganic Compounds*; Roundhill, D. M.; Fackler, J. P., Jr., Eds.; Plenum: New York, 1999; pp 1−27. (g) Shi, S. In *Optoelectronic Properties of Inorganic Compounds*; Roundhill, D. M.; Fackler, J. P., Jr., Eds.; Plenum: New York, 1999; pp 55−105. (h) Le Bozec, H.; Renouard, T. *Eur. J. Inorg. Chem.* **2000**, 229. (i) Barlow, S.; Marder, S. R. *Chem. Commun*. **2000**, 1555. (j) Lacroix, P. G. *Eur. J. Inorg. Chem*. **2001**, 339. (k) Di, Bella, S. *Chem. Soc. Rev.* **2001**, *30*, 355. (l) Coe, B. J. In *Comprehensive Coordination Chemistry II*; McCleverty, J. A., Meyer, T. J., Eds.; Elsevier Pergamon: Oxford, U.K., 2004; Vol. 9, pp 621−687. (m) Cariati, E.; Pizzotti, M.; Roberto, D.; Tessore, F.; Ugo, R. *Coord. Chem. Rev.* **2006**, *250*, 1210. (n) Coe, B. J. *Acc. Chem. Res.* **2006**, *39*, 383.

(3) (a) Coe, B. J.; Houbrechts, S.; Asselberghs, I.; Persoons, A. *Angew. Chem., Int. Ed.* **1999**, *38*, 366. (b) Weyland, T.; Ledoux, I.; Brasselet, S.; Zyss, J.; Lapinte, C. *Organometallics* **2000**, *19*, 5235. (c) Malaun, M.; Reeves, Z. R.; Paul, R. L.; Jeffery, J. C.; McCleverty, J. A.; Ward, M. D.; Asselberghs, I.; Clays, K.; Persoons, A. *Chem. Commun*. **2001**, 49. (d) Malaun, M.; Kowallick, R.; McDonagh, A. M.; Marcaccio, M.; Paul, R. L.; Asselberghs, I.; Clays, K.; Persoons, A.; Bildstein, B.; Fiorini, C.; Nunzi, J.-M.; Ward, M. D.; McCleverty, J. A. *J. Chem. Soc., Dalton Trans.* **2001**, 3025. (e) Cifuentes, M. P.; Powell, C. E.; Humphrey, M. G.; Heath, G. A.; Samoc, M.; Luther-Davies, B. *J. Phys. Chem. A* **2001**, *105*, 9625. (f) Paul, F.; Costuas, K.; Ledoux, I.; Deveau, S.; Zyss, J.; Halet, J.-F.; Lapinte, C. *Organometallics* **2002**, *21*, 5229. (g) Powell, C. E.; Cifuentes, M. P.; Morrall, J. P.; Stranger, R.; Humphrey, M. G.; Samoc, M.; Luther-Davies, B.; Heath, G. A. *J. Am. Chem. Soc.* **2003**, *125*, 602. (h) Asselberghs, I.; Clays, K.; Persoons, A.; McDonagh, A. M.; Ward, M. D.; McCleverty, J. A. *Chem. Phys. Lett.* **2003**, *368*, 408. (i) Powell, C. E.; Humphrey, M. G.; Cifuentes, M. P.; Morrall, J. P.; Samoc, M.; Luther-Davies, B. *J. Phys. Chem. A* **2003**, *107*, 11264. (j) Sporer, C.; Ratera, I.; Ruiz-Molina, D.; Zhao, Y.-X.; Vidal-Gancedo, J.; Wurst, K.; Jaitner, P.; Clays, K.; Persoons, A.; Rovira, C.; Veciana, J. *Angew. Chem., Int. Ed.* **2004**, *43*, 5266.

(4) Selected examples: (a) He, G. S.; Lin, T.-C.; Prasad, P. N.; Cho, C.-C.; Yu, L.-J. *Appl. Phys. Lett.* **2003**, *82*, 4717. (b) Yang, Z.; Wu, Z.-K.; Ma, J.-S.; Xia, A.-D.; Li, Q.-S.; Liu, C.-L.; Gong, Q.-H. *Appl. Phys. Lett.* **2005**, *86*, 061903. (c) Wang, C.; Wang, X.-M.; Shao, Z.-S.; Zhao, X.; Zhou, G.-Y.; Wang, D.; Fang, Q.; Jiang, M.-H. *Appl. Opt.* **2001**, *40*, 2475. (d) Zheng, Q.-D.; He, G. S.; Lin, T.-C.; Prasad, P. N. *J. Mater. Chem.* **2003**, *13*, 2499. (e) Bhawalkar, J. D.; Kumar, N. D.; Zhao, C. F.; Prasad, P. N. *J. Clin. Laser Med. Surg.* **1997**, *15*, 201.

(5) Selected examples: (a) Lee, W.-H.; Lee, H.-C.; Kim, J.-A.; Choi, J.-H.; Cho, M.-H.; Jeon, S.-J.; Cho, B. R. *J. Am. Chem. Soc.* **2001**, *123*, 10658. (b) Beljonne, D.; Wenseleers, W.; Zojer, E.; Shuai, Z.-G.; Vogel, H.; Pond, S. J. K.; Perry, J. W.; Marder, S. R.; Bredas, J.-L. *Adv. Funct. Mater.* **2002**, *12*, 631. (c) Kannan, R.; He, G. S.; Lin, T.-C.; Prasad, P. N.; Vaia, R. A.; Tan, L.-S. *Chem. Mater.* **2004**, *16*, 185. (d) Ray, P. C.; Leszczynski, J. *J. Phys. Chem. A* **2005**, *109*, 6689. (e) Zhou, X.; Feng, J.-K.; Ren, A.-M. *Chem. Phys. Lett.* **2005**, *403*, 7.

(6) (a) Kawamata, J.; Ogata, Y.; Yamagishi, A. *Mol. Cryst. Liq. Cryst. Sci. Technol., Sect. A* **2002**, *379*, 389. (b) Hurst, S. K.; Humphrey, M. G.; Isoshima, T.; Wostyn, K.; Asselberghs, I.; Clays, K.; Persoons, A.; Samoc, M; Luther-Davies, B. *Organometallics* **2002**, *21*, 2024. (c) Das, S.; Nag, A.; Goswami, D.; Bharadwaj, P. K. *J. Am. Chem. Soc.* **2006**, *128*, 402.

(7) Liu, X.-J.; Feng, J.-K.; Ren, A.-M.; Cheng, H.; Zhou, X. *J. Chem. Phys.* **2004**, *120*, 11493.

(8) Coe, B. J.; Harris, J. A.; Brunschwig, B. S.; Asselberghs, I.; Clays, K.; Garín, J.; Orduna, J. *J. Am. Chem. Soc.* **2005**, *127*, 13399.

(9) Chichak, K.; Branda, N. R. *Chem. Commun.* **2000**, *1211*.

(10) (a) Sheik-Bahae, M.; Said, A. A.; van Stryland, E. W. *Opt. Lett.* **1989**, *14*, 955. (b) Sheik-Bahae, M.; Said, A. A.; Wei, T. H.; Hagan, D. J.; van Stryland, E. W. *IEEE J. Quantum Electron.* **1990**, *26*, 760. (c) van Stryland, E. W.; Sheik-Bahae, M. *Opt. Eng.* **1998**, *60*, 655.

(11) Frisch, M. J.; Trucks, G. W.; Schlegel, H. B.; Scuseria, G. E.; Robb, M. A.; Cheeseman, V. G.; Montgomery, J. A., Vreven, Jr. T.; Kudin, K. N.; Burant, J. C.; Millam, J. M.; Iyengar, S. S.; Tomasi, J.; Barone, V.; Mennucci, B.; Cossi, M.; Scalmani, G.; Rega, N.; Petersson, G. A.; Nakatsuji, H.; Hada, M.; Ehara, M.; Toyota, K.; Fukuda, R.; Hasegawa, J.; Ishida, M.; Nakajima, T.; Honda, Y.; Kitao, O.; Nakai, H.; Klene, M.; Li, X.; Knox, J. E.; Hratchian, H. P.; Cross, J. B.; Adamo, C.; Jaramillo, J.; Gomperts, R.; Stratmann, R. E.; Yazyev, O.; Austin, A. J.; Cammi, R.; Pomelli, C.; Ochterski, J. W.; Ayala, P. Y.; Morokuma, K.; Voth, G. A.; Salvador, P.; Dannenberg, J. J.; Zakrzewski, V. G.; Dapprich, S.; Daniels, A. D.; Strain, M. C.; Farkas, O.; Malick, D. K.; Rabuck, A. D.; Raghavachari, K.; Foresman, J. B.; Ortiz, J. V.; Cui, Q.; Baboul, A. G.; Clifford, S.; Cioslowski, J.; Stefanov, B. B.; Liu, G.; Liashenko, A.; Piskorz, P.; Komaromi, I.; Martin, R. L.; Fox, D. J.; Keith, T.; Al-Laham, M. A.; Peng, C. Y.; Nanayakkara, A.; Challacombe, M.; Gill, P. M. W.; Johnson, B.; Chen, W.; Wong, M. W.; Gonzalez, C.; Pople, J. A.; *Gaussian 03*, Revision B.05; Gaussian, Inc.: Pittsburgh, PA, 2003.

(12) (a) Pople, J. A.; Beveridge, D. L.; Dobosh, P. A. *J. Chem. Phys.* **1967**, *47*, 2026. (b) Ridley, J.; Zerner, M. *Theor. Chim. Acta* **1973**, *32*, 111.

(13) Mataga, N.; Nishimoto, K. *Z. Phys. Chem.* **1957**, *13*, 140.

(14) Buenker, R. J.; Peyerimhoff, S. D. *Theor. Chim. Acta* **1974**, *35*, 33.

(15) (a) Zhou, X.; Ren, A. M.; Feng, J. K.; Liu, X. J. *J. Phys. Chem. A* **2003**, *107*, 1850. (b) Zhou, X.; Ren, A. M.; Feng, J. K.; Liu, X. J. *Chem. Phys. Lett.* **2003**, *373*, 167.

(16) (a) Zojer, E.; Beljonne, D.; Kogej, T.; Vogel, H.; Marder, S. R.; Perry, J. W.; Brédas, J.-L. *J. Chem. Phys.* **2002**, *116*, 3646. (b) Beljonne, D.; Wenseleers, W.; Zojer, E.; Shuai, Z.; Vogel, H.; Pond, S. J. K.; Perry, J. W.; Marder, S. R.; Brédas, J.-L. *Adv. Funct. Mater.* **2002**, *12*, 631. (c) Zojer, E.; Wenseleers, W.; Pacher, P.; Barlow, S.; Halik, M.; Grasso, C.; Perry, J. W.; Marder, S. R.; Brédas, J.-L. *J. Phys. Chem. B* **2004**, *108*, 8641.

(17) Luo, Y.; Norman, P.; Macak, P.; Agren, H. *J. Phys. Chem. A* **2000**, *104*, 4718.

(18) Anderson, R. J.; Holtom, G. R.; McClain, W. M. *J. Chem. Phys.* **1979**, *70*, 4310.

(19) Selected recent examples of chromophores with large σ_2 values: (a) Drobizhev, M.; Stepanenko, Y.; Dzenis, Y.; Karotki, A.; Rebane, A.; Taylor, P. N.; Anderson, H. L. *J. Am. Chem. Soc.* **2004**, *126*, 15352. (b) Beverina, L.; Fu, J.; Leclercq, A.; Zojer, E.; Pacher, P.; Barlow, S.; van

Stryland, E. W.; Hagan, D. J.; Brédas, J.-L.; Marder, S. R. *J. Am. Chem. Soc.* **2005**, *127*, 7282. (c) Chung, S .J.; Rumi, M.; Alain, V.; Barlow, S.; Perry, J. W.; Marder, S. R. *J. Am. Chem. Soc.* **2005**, *127*, 10844. (d) Lee, S. K.; Yang, W. J.; Choi, J. J.; Kim, C. H.; Jeon, S. J.; Cho, B. R. *Org. Lett.* **2005**, *7*, 323. (e) Chung, S. J.; Rumi, M.; Alain, V.; Barlow, S.; Perry, J. W.; Marder, S. R. *J. Am. Chem. Soc.* **2005**, *127*, 10844. (f) Misra, R.; Kumar, R.; Chandrashekar, T. K.; Nag, A.; Goswami, D. *Org. Lett.* **2006**, *8*, 629.

(20) Orr, B. J.; Ward, J. F. *Mol. Phys.* **1971**, *20*, 513.

(21) For examples, see: (a) Dhenaut, C.; Ledoux, I.; Samuel, I. D. W.; Zyss, J.; Bourgault, M.; Le Bozec, H. *Nature* **1995**, *374*, 339. (b) Le Bozec, H.; Renouard, T.; Bourgault, M.; Dhenaut, C.; Brasselet, S.; Ledoux, I.; Zyss, J. *Synth. Met.* **2001**, *124*, 185. (c) Maury, O.; Viau, L.; Sénéchal, K.; Corre, B.; Guégan, J.-P.; Renouard, T.; Ledoux, I.; Zyss, J.; Le Bozec, H. *Chem.—Eur. J.* **2004**, *10*, 4454. (d) Maury, O.; Le Bozec, H. *Acc. Chem. Res.* **2005**, *38*, 691.

(22) Baev, A.; Prasad, P. N.; Samoc, M. *J. Chem. Phys.* **2005**, *122*, 224309-1-6.